

The solubility of Ba in a new Cs waste form, $\text{Cs}_2\text{TiNb}_6\text{O}_{18}$

Day, George; Cutts, Geoffrey L.; Chen, Tzu Yu; Hriljac, Joseph A.; Guo, Yina

DOI:
[10.1557/adv.2017.52](https://doi.org/10.1557/adv.2017.52)

License:
None: All rights reserved

Document Version
Peer reviewed version

Citation for published version (Harvard):
Day, G, Cutts, GL, Chen, TY, Hriljac, JA & Guo, Y 2017, 'The solubility of Ba in a new Cs waste form, $\text{Cs}_2\text{TiNb}_6\text{O}_{18}$ ', *MRS Advances*, vol. 2, no. 13, pp. 723-728. <https://doi.org/10.1557/adv.2017.52>

[Link to publication on Research at Birmingham portal](#)

Publisher Rights Statement:
Checked for eligibility 09/10/2018

First published in MRS Advances
<https://doi.org/10.1557/adv.2017.52>

General rights

Unless a licence is specified above, all rights (including copyright and moral rights) in this document are retained by the authors and/or the copyright holders. The express permission of the copyright holder must be obtained for any use of this material other than for purposes permitted by law.

- Users may freely distribute the URL that is used to identify this publication.
- Users may download and/or print one copy of the publication from the University of Birmingham research portal for the purpose of private study or non-commercial research.
- User may use extracts from the document in line with the concept of 'fair dealing' under the Copyright, Designs and Patents Act 1988 (?)
- Users may not further distribute the material nor use it for the purposes of commercial gain.

Where a licence is displayed above, please note the terms and conditions of the licence govern your use of this document.

When citing, please reference the published version.

Take down policy

While the University of Birmingham exercises care and attention in making items available there are rare occasions when an item has been uploaded in error or has been deemed to be commercially or otherwise sensitive.

If you believe that this is the case for this document, please contact UBIRA@lists.bham.ac.uk providing details and we will remove access to the work immediately and investigate.

The Solubility of Ba in a New Cs Waste Form, $\text{Cs}_2\text{TiNb}_6\text{O}_{18}$

George Day¹, Geoffrey L. Cutts¹, Tzu-Yu Chen¹, Joseph A. Hriljac¹ and Yina Guo²

¹ School of Chemistry, University of Birmingham, Edgbaston, Birmingham, B15 2TT, UK

² Materials and Surface Science Institute, University of Limerick, Sreelane, Limerick, Ireland

ABSTRACT

We report experimental and computational studies of Ba doping for Cs in $\text{Cs}_2\text{TiNb}_6\text{O}_{18}$, a material with potential to be an exceptional ceramic wastefrom for Cs sequestration. Three co-doping (simultaneous metal reduction for charge balance of Ba^{2+} for Cs^+) schemes have been experimentally tested: Ti^{4+} for Nb^{5+} , Ti^{3+} for Ti^{4+} and Nb^{4+} for Nb^{5+} . Unfortunately, none showed conclusively that the co-substitution was successful. Atomistic modelling was then performed on all three schemes using novel potentials to assess the energetic feasibility, from these the most favourable scenario is reduction of Nb^{5+} to Nb^{4+} .

INTRODUCTION

^{137}Cs is one of the most problematic radionuclides formed from the nuclear fission process. It is one of the primary heat and radioactivity contributors in spent fuel with a half-life of 30.2 years and a fission yield of around 6 %. Furthermore, many salts of Cs are highly soluble and therefore Cs becomes readily mobile if released into the biosphere. As a result of these characteristics, Cs is often separated from waste streams using a number of different processes and materials, typically ion exchange with inorganic exchangers. Inorganic exchangers are often employed on account of their high selectivity towards Cs, radioactivity and heat resistance and compatibility to be converted into a final waste form.

Hot isostatically pressing (HIPing) Cs-loaded IONSIV produces a robust Cs waste form, $\text{Cs}_2\text{TiNb}_6\text{O}_{18}$ [1]. This has been shown to have comparable leaching properties to hollandite, the Cs-containing phase in SYNROC [2]. When considering Cs waste forms, it is important to know if $^{137}\text{Ba}^{2+}$, the transmutation product of $^{137}\text{Cs}^+$, can be retained. By demonstrating the successful synthesis of mixed Cs/Ba hollandites, it has been claimed in previous studies that this process will occur naturally in hollandites [3]. Therefore synthesis of Ba doped $\text{Cs}_2\text{TiNb}_6\text{O}_{18}$ could provide evidence that Ba could be retained and give reassurance of the long term integrity of the waste form. It was thought that Ba incorporation could be achieved via three stoichiometric mechanisms:

- Scheme 1: $\text{Cs}_{2-x}\text{Ba}_x\text{Ti}_{1+x}\text{Nb}_{6-x}\text{O}_{18}$
- Scheme 2: $\text{Cs}_{2-x}\text{Ba}_x\text{Ti}_x^{3+}\text{Ti}_{1-x}^{4+}\text{Nb}_6\text{O}_{18}$
- Scheme 3: $\text{Cs}_{2-x}\text{Ba}_x\text{TiNb}_x^{4+}\text{Nb}_{6-x}^{5+}\text{O}_{18}$

Scheme 1 served only as a ‘proof of concept’ as is not a realistic scenario in a waste form. Scheme 2 and 3 however represented ‘real life’ scenarios where Cs^+ decays to Ba^{2+} , releasing a β^- particle which subsequently reduces either Ti^{4+} to Ti^{3+} (scheme 2) or Nb^{5+} to Nb^{4+} (scheme 3). A series of samples following schemes 1, 2 and 3 have been synthesized and analyzed.

EXPERIMENT

Samples were prepared through traditional solid state methods. Multiple firings at 1200 °C were required to complete the reaction. Air sensitive samples were prepared in an inert atmosphere and fired in evacuated sealed quartz tubes to prevent oxidation of the unstable cations. Powder X-ray diffraction (XRD) experiments were carried out using a Bruker D8 Advance diffractometer using Cu $K_{\alpha 1}$ ($\lambda = 1.5406 \text{ \AA}$) radiation in transmission mode, equipped with a Lynx Eye Si-strip detector. Data was collected in the 2θ range from 5° to 85° and 22° to 38° at a step size of 0.0198° . Rietveld analysis of XRD data was performed using the EXPGUI GSAS suite [4,5]. Elemental analysis was carried out using a Bruker S8 Tiger Wavelength Dispersive X-ray Fluorescence spectrometer. TEM data was collected using a JEOL JEM-2100F equipped with a SEI/BSE detector, operating at 200 kv in STEM mode. Buckingham potentials for the computational work were empirically derived using a code previously developed by the group based on Reverse Monte Carlo (RMC) methodology [6]. Static calculations have been carried out using the General Utility Lattice Program (GULP) code [7].

DISCUSSION

Inspection of the XRD data confirmed that the pure $\text{Cs}_2\text{TiNb}_6\text{O}_{18}$ is trigonal and crystallizes in the $P\bar{3}m1$ space group, $a = 7.53$ and $c = 8.19 \text{ \AA}$ (figure 1, a). Early attempts of Ba doping were carried out following scheme 1 and samples were synthesized to the formulae $\text{Cs}_{2-x}\text{Ba}_x\text{Ti}_{1+x}\text{Nb}_{6-x}\text{O}_{18}$ ($x=0.3$ and 0.6). Substituting excess Ti^{4+} for Nb^{5+} not only provided the required charge balance to achieve Ba doping, but also posed the easiest synthetic route. At these levels of Ba doping, $\text{Ba}_2\text{Ti}_3\text{Nb}_4\text{O}_{18}$ is observed in the XRD patterns and this was quantified via Rietveld refinements (figures 1 and 2). The values from the weight fraction analysis suggest that the Ba almost entirely resides in the impurity phase (table 1).

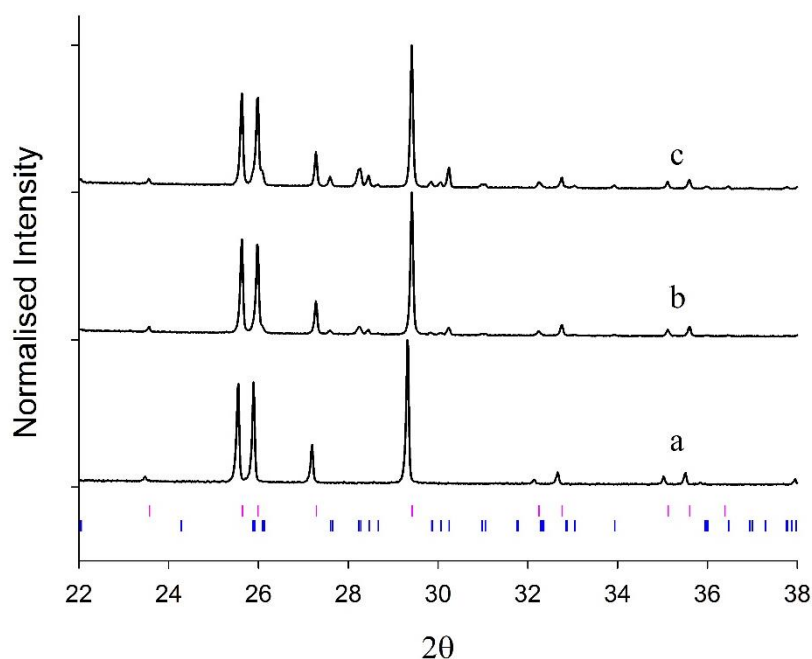


Figure 1. XRD stack plot of (a) $\text{Cs}_2\text{TiNb}_6\text{O}_{18}$, (b) $\text{Cs}_{1.7}\text{Ba}_{0.3}\text{Ti}_{1.3}^{4+}\text{Nb}_{5.7}\text{O}_{18}$ and (c) $\text{Cs}_{1.4}\text{Ba}_{0.6}\text{Ti}_{1.6}^{4+}\text{Nb}_{5.4}\text{O}_{18}$. Top ticks: $\text{Cs}_2\text{TiNb}_6\text{O}_{18}$ (ICDD PDF 04-012-7437), lower ticks: $\text{Ba}_2\text{Ti}_3\text{Nb}_4\text{O}_{18}$ (ICDD PDF 01-073-6191).

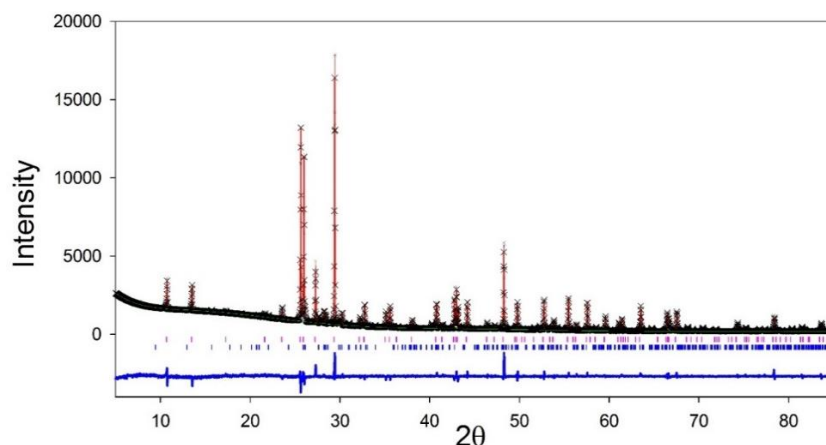


Figure 2. Rietveld refinement $\text{Cs}_{1.7}\text{Ba}_{0.3}\text{Ti}_{1.3}\text{Nb}_{5.7}\text{O}_{18}$ showing the observed (crosses), calculated (top line) and difference (lower line) patterns as well as positions of allowed reflections for the main phase (upper) and impurity phase (lower).

Table 1. Rietveld refinement results for $\text{Cs}_{2-x}\text{Ba}_x\text{Ti}_{1+x}\text{Nb}_{6-x}\text{O}_{18}$ ($x=0.3$ and 0.6).

x	Target wt% Ba incorporation	wt% $\text{Cs}_2\text{TiNb}_6\text{O}_{18}$	wt% $\text{Ba}_2\text{Ti}_3\text{Nb}_4\text{O}_{18}$	% Ba in impurity
0.3	3.6	86.407(4)	13.59(3)	3.5
0.6	7.3	71.786(8)	28.21(2)	7.2

Having identified impurities for the higher doped samples, a series of lower level Ba samples were synthesized following scheme 1 to determine if any Ba solubility is possible. XRF results are consistent with the expected level of doping but analysis of the XRD data again confirmed impurity peaks that were assigned to $\text{BaTi}_3\text{Nb}_4\text{O}_{17}$ and $\text{BaTiNb}_4\text{O}_{13}$ (figure 3). To better represent ‘real life’ scenarios, samples were also synthesized following schemes 2 and 3 and again the XRD patterns contain impurities (figure 4).

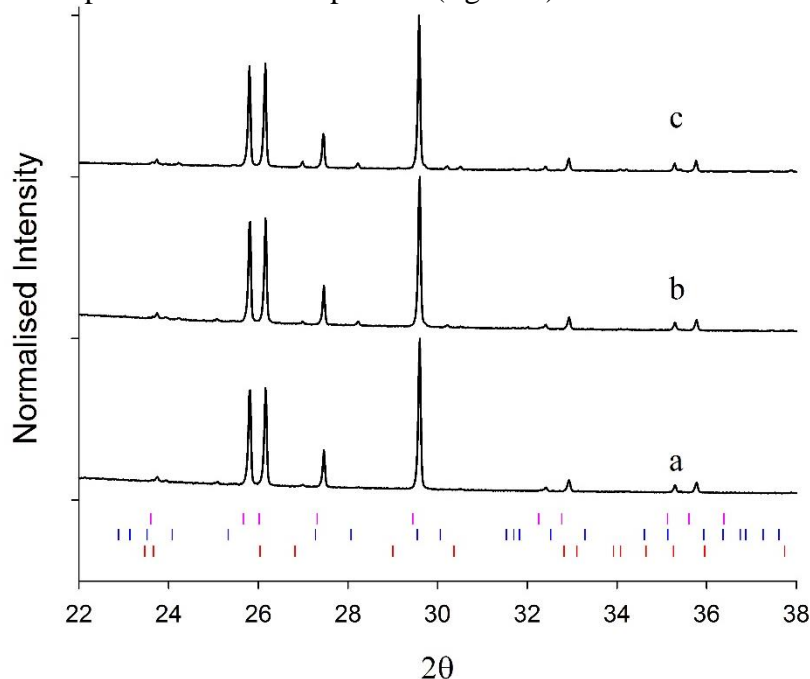


Figure 3. XRD stack plot $\text{Cs}_{2-x}\text{Ba}_x\text{Ti}_{1+x}\text{Nb}_{6-x}\text{O}_{18}$ (a) $x = 0.05$, (b) $x = 0.10$ and (c) $x = 0.15$. Top ticks $\text{Cs}_2\text{TiNb}_6\text{O}_{18}$, middle ticks $\text{BaTiNb}_4\text{O}_{13}$ (ICDD PDF 04-009-2510) and lower ticks $\text{BaTi}_3\text{Nb}_4\text{O}_{17}$ (ICDD PDF 00-038-1482).

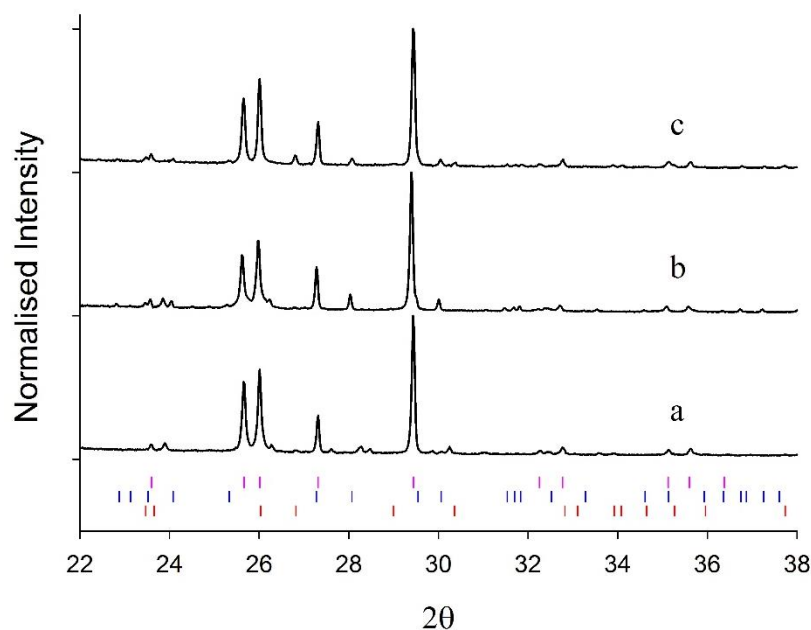


Figure 4. XRD stack plot of (a) $Cs_{1.8}Ba_{0.2}Ti_{1.2}Nb_{5.8}O_{18}$, (b) $Cs_{1.8}Ba_{0.2}Ti_{0.2}^{3+}Ti_{0.8}^{4+}Nb_6O_{18}$ and (c) $Cs_{1.8}Ba_{0.2}TiNb_{0.2}^{4+}Nb_{5.8}^{5+}O_{18}$, (schemes 1, 2 and 3 for $x = 0.2$). Top ticks $Cs_2TiNb_6O_{18}$, middle ticks $BaTiNb_4O_{13}$ and lower ticks $BaTi_3Nb_4O_{17}$.

To further investigate if any Ba resides in nominally doped $Cs_2TiNb_6O_{18}$, elemental analyses were carried out in TEM/EDS. (table 2, figure 5). The dark-field TEM image (figure 4b) and EDS results (table 2) show that points A and C appear to be on the same crystal of $Cs_2TiNb_6O_{18}$. Point B shows a Ba-rich particle on the surface of the $Cs_2TiNb_6O_{18}$ crystal. The Ba content of point B can be estimated by subtracting an average of the values from points A and C from that of B. The residual suggests that Ba almost entirely resides in the impurity particle, in this case likely a barium titanium niobate. This study is not entirely conclusive, however this coupled with the X-ray data strongly indicates that Ba does not incorporate into the target phase.

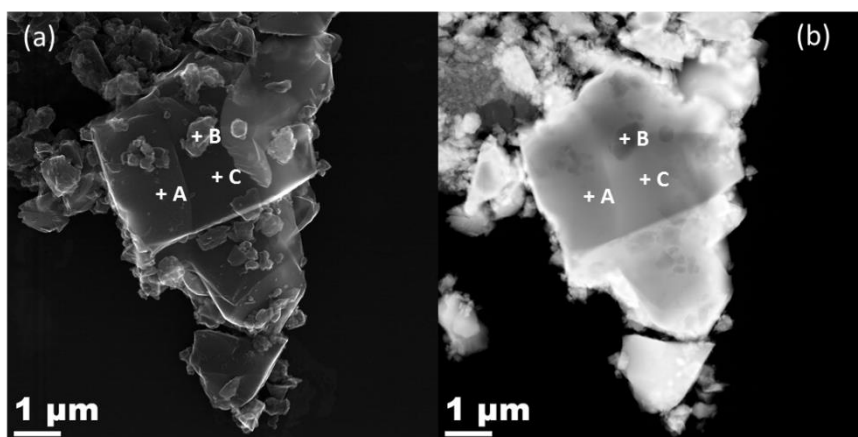


Figure 5. TEM image of $Cs_{1.9}Ba_{0.1}Ti_{1.1}Nb_{5.9}O_{18}$ (a) secondary electron image (b) dark-field image. + marks the points for EDS analysis.

Table 2. Multi-point analysis of $\text{Cs}_{1.9}\text{Ba}_{0.1}\text{Ti}_{1.1}\text{Nb}_{5.9}\text{O}_{18}$ using TEM/EDS.

	CsL	BaL		TiK		NbK	
	at%	at%	At. Ratio (to Cs)	at%	At. Ratio (to Cs)	at%	At. Ratio (to Cs)
Point A	22.8	1.9	0.08	8.1	0.35	46.3	2.03
Point B	8.0	28.8	3.61	13.0	1.63	37.3	4.68
Point C	24.8	2.0	0.08	9.2	0.37	49.7	2.00
Residual*			3.53		2.03		2.47

* Residual elements after subtracting equal amount of those of average point A and C.

Computational

Having been unable to confirm any level of Ba doping experimentally, calculations have been carried out using the GULP code [7] to investigate the energetics of different mechanisms associated with Ba doping. A set of novel potentials have been empirically derived using a RMC methodology (table 3) [6].

Table 3. Buckingham Potentials used in the calculations.

Interaction	A / eV	ρ / Å	C / eV·Å ⁶	R _{cut} / Å
Cs ^{0.66} core O ^{-1.32} core	48865.05797	0.24566	178.45697	10
Ti ^{2.64} core O ^{-1.32} core	5910.02993	0.24483	70.37101	10
Nb ^{3.3} core O ^{-1.32} core	7627.35101	0.22762	2.143220	10
Ba ^{1.32} core O ^{-1.32} core	14978.09895	0.25091	9.44896	10
Ti ^{1.98} core O ^{-1.32} core	1325.89734	0.29404	96.85703	10
Nb ^{2.64} core O ^{-1.32} core	7882.42419	0.24021	120.97084	10
O ^{-1.32} core O ^{-1.32} core	2065.02360	0.31729	110.89703	12

Defects in the $\text{Cs}_2\text{TiNb}_6\text{O}_{18}$ system have been approximated at infinite dilution and as clusters using the Mott-Littleton (two-region) approach [8]. There are two crystallographic sites for the Ti/Nb, site 1 at (0, 0, 0.5) and site 2 at (0.17, 0.17, 0.1457). Analysis of defect calculations via the Mott-Littleton method suggests that the charge compensation cation prefers to be on site 2 and that also the defect pairs prefer to cluster together as indicated by the negative binding energies (table 4).

Table 4. Scheme/Site energy compensation preference and binding energies.

Scheme	Site Preference	Energy Difference between sites / eV	Binding Energy/eV
$\text{Cs}_{2-x}\text{Ba}_x\text{Ti}_{1+x}\text{Nb}_{6-x}\text{O}_{18}$, scheme 1	2	≈ 0.5	-0.4
$\text{Cs}_{2-x}\text{Ba}_x\text{Ti}^{3+}_x\text{Ti}^{4+}_{1-x}\text{Nb}_6\text{O}_{18}$, scheme 2	2	≈ 0.3	-0.3
$\text{Cs}_{2-x}\text{Ba}_x\text{TiNb}^{4+}_x\text{Nb}^{5+}_{6-x}\text{O}_{18}$, scheme 3	2	≈ 0.5	-0.4

Solution energies have been calculated using both the Mott Littleton method and the Monte Carlo Markov Chain (MCMC) supercell method (table 5). The supercells for the MCMC

method were doped to 20% conversion of Cs to Ba. The solution energies from the supercell method better simulate Ba doping in the $\text{Cs}_2\text{TiNb}_6\text{O}_{18}$ system and the positive solution energies for all schemes suggest that Ba incorporation is unfavorable which supports the experimental studies.

Table 5. Solution energies for the three schemes.

Scheme	Mott-Littleton / eV	Supercell Method / eV
1	3.95	3.49
2	1.05	3.12
3	-3.46	2.76

CONCLUSIONS

Attempts have been carried out both synthetically and theoretically to incorporate Ba into a new Cs waste form $\text{Cs}_2\text{TiNb}_6\text{O}_{18}$. Experimental doping of Ba was not achieved via any of the proposed charge compensation schemes and Ba impurity phases were identified from XRD and TEM studies as $\text{Ba}_2\text{Ti}_3\text{Nb}_4\text{O}_{18}$, $\text{BaTiNb}_4\text{O}_{13}$ and $\text{BaTi}_3\text{Nb}_4\text{O}_{17}$. Simulations using the GULP code supported the experimental studies, suggesting that at least thermodynamically, it is unfavourable to dope Ba into $\text{Cs}_2\text{TiNb}_6\text{O}_{18}$ via all three charge compensation schemes.

ACKNOWLEDGMENTS

We acknowledge funding from the School of Chemistry for scholarship support (GD, GLC) and the EPSRC via a DTP scholarship grant (GLC) and DISTINCTIVE (EP/L014041/1). The Bruker D8 and S8 instruments used in this research were obtained through Birmingham Science City: Creating and Characterizing Next Generation Advanced Materials (West Midlands Centre for Advanced Materials Project 1), with support from Advantage West Midlands and partially funded by the European Regional Development Fund. The Advanced Materials Facility is part of the Centre for Chemical and Materials Analysis in the School of Chemistry at the University of Birmingham. Data associated with the results shown in this paper are accessible from the University of Birmingham Archive: <http://epapers.bham.ac.uk/2228/>.

REFERENCES

1. T.-Y. Chen, J. A. Hriljac, A. S. Gandy, M. C. Stennett, N. C. Hyatt and E. R. Maddrell, *Scientific Basis for Nuclear Waste Management XXXVI, MRS Symp. Proc.* **1518**, 67-72 (2013).
2. A. Ringwood, *Mineralogical Magazine*. **49**, 159-176 (1985).
3. A. Y. Leinekugel-le-Cocq, P. Deniard, S. Jobic, R. Cerny, F. Bart, and H. Emerich, *J. Solid State Chem.* **179**, 3196–3208 (2006).
4. A.C. Larson and R.B. Von Dreele, "General Structure Analysis System (GSAS)", Los Alamos National Laboratory Report LAUR 86-748 (2000).
5. B. H. Toby, *EXPGUI*, a graphical user interface for GSAS, *Journal of Applied Crystallography*. **34**, 210-213 (2001).
6. Geoffrey Cutts, PhD thesis, University of Birmingham.
7. J. D. Gale and A. L. Rohl, *Molecular Simulation*. **29**, 291–341 (2003).
8. F. N. Mott and M. J. Littleton, *Transactions of the Faraday Society* **34**, 485-499 (1938).